Dalton Transactions

Accepted Manuscript

ROYAL SOCIETY OF CHEMISTRY

rsc.li/dalton

ROYAL SOCIETY OF CHEMISTRY View Article Online
DOI: 10.1039/C8DT04689A

Journal Name

ARTICLE

O–H and (CO)N–H bond weakening by coordination to Fe(II)

Sandra Resa,[a] Alba Millán,[a,*] Noelia Fuentes,[b] Luis Crovetto,[c] M. Luisa Marcos,[d] Luis Lezama,[e] Duane Choquesillo-Lazarte,[f] Victor Blanco,[a] Araceli G. Campaña,[a] Diego J. Cárdenas[b,*] and Juan M. Cuerva[a,*]

Received 00th January 20xx,
Accepted 00th January 20xx

DOI: 10.1039/x0xx00000x

www.rsc.org/

New *N,N'*-dimethyl-*N,N'*-bis(2-pyridylmethyl)-ethane-1,2-diamine derivatives bearing covalently linked OH and (CO)NH groups have been synthesized. The coordination of those pendant hydroxyl/amide groups to a Fe(II) metal center is demonstrated both in solution, even in the presence of chloride as counterion, and in solid state, by means of X-ray diffraction crystal structures. As a result of this coordination, the experimental bond dissociation free energies (BDFE) of O–H and (CO)N–H bonds are remarkably diminished down to 76.0 and 80.5 kcal mol^{-1} respectively, which is also in agreement with DFT-based theoretical calculations. Those BDFE values are in the range of commonly used hydrogen-atom donor reagents. The strategy presented here allows an unequivocal evaluation of the influence of metal coordination in X–H bond weakening in organic solvents which could be easily extended to other metal centers.

Introduction

O–H bonds in alcohols and water are among the strongest covalent bonds, showing bond dissociation free energies (BDFE) ranging from 122.7 (water) to 100.8 (EtOH) kcal mol^{-1}.[1] The energy of this bond formation is the driving force of many biological and biomimetic oxidation processes of simple alkanes (C–H BDFEs ranging from 106 to 88.3 kcal mol^{-1}) and phenols (O–H BDFEs ranging from 95.5 to 73.8 kcal mol^{-1}) by the corresponding metal hydroxides and oxides.[2] A classic example is the use of iron hydroxides/oxides in high oxidation state to generate the corresponding aqua/hydroxide complexes, as exemplified in many natural occurring processes (Figure 1, left to right). Thus for example, this transformation is essential in the proper functioning of *Escherichia coli* ribonucleotide reductase, in which tyrosine (Y122) is oxidized by an Fe(III)-hydroxide, yielding coordinated water (W48) to a Fe(III)/Fe(IV) cluster.[3] Iron aqua and hydroxo complexes[4] are also involved in the PCET processes in the oxidation of ferullic acid by horseradish peroxydase[5] or radical initiation in class I ribonucleotide reductase.[6,7] Hydroxo or aquocomplexes of manganese/iron clusters have been also identified as cofactors in *Chlamydia trachomatis*[8] and *Mycobacterium tuberculosis*[9] ribonucleotide reductase.

Less frequent is the opposite transformation in which the BDFE energy of O–H bonds is considerably diminished by coordination to a metal, thus transforming the corresponding O–H bonds in potential hydrogen donors (Figure 1, right to left). A key example is the behaviour of water coordinated to manganese cluster in photosystem II (PSII). A hydrogen-atom transfer from coordinated water molecules to a tyrosine (Yz) radical is proposed as the responsible of a sequential electron and proton draining in O_2 production by photosynthesis.[10-12] In that situation, the BDFE of the coordinated water must be similar or even lower than BDE/BDFE of tyrosine (BDE = 86 kcal mol^{-1}, BDFE = 87.8 kcal mol^{-1}).[1] Experimental and theoretical BDE values of water[13,14] and hydroxy[15] manganese model complexes showed that the values ranges between 77 and 94 kcal mol^{-1}, fitting with the original proposal. In fact, this ability of manganese to diminish the BDE of proximal OH groups has been considered in the heart of the PSII evolutionary success.[16]

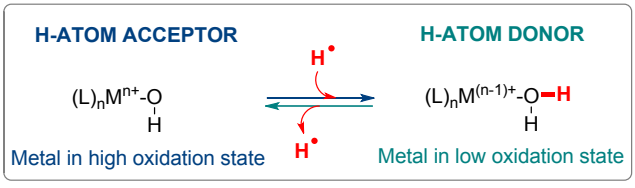

Figure 1. Metal hydroxide or aqua complexes as hydrogen atom acceptor or donor.

Within this context, we and other groups have recently shown that the reactivity of Ti(III)[17] or Sm(II)[18] towards carbon-centered radicals in the presence of water and methanol can only be explained assuming a considerably diminishing of the O–H bond dissociation energy after coordination to such low

[a] Departamento Química Orgánica, Universidad de Granada (UGR). Avda. Fuentenueva, s/n, 18071 Granada, Spain. E-mail: jmcuerva@ugr.es
[b] Departamento de Química Orgánica, Universidad Autónoma de Madrid. Ciudad Universitaria de Cantoblanco, 28049 Madrid, Spain.
[c] Departamento de Fisicoquímica, Facultad de Farmacia, (UGR). Cartuja Campus, 18071 Granada, Spain.
[d] Departamento de Química, Universidad Autónoma de Madrid. Ciudad Universitaria de Cantoblanco, 28049 Madrid, Spain.
[e] Departamento de Química Inorgánica, Facultad de Ciencia y Tecnología, Universidad del País Vasco, UPV/EHU, 48940 Leioa, Spain
[f] Laboratorio de Estudios Cristalográficos, Instituto Andaluz de Ciencias de la Tierra (CSIC-UGR), 18100 Armilla, Granada, Spain.

† Electronic Supplementary Information (ESI) available: synthesis and NMR spectra of ligands and iron (II) complexes, magnetic susceptibility graphics, UV-Vis titration spectra, voltammograms, crystallographic data and atomic coordinates for DFT calculations. CCDC 1880891-1880897. For ESI and crystallographic data in CIF or other electronic format see DOI: 10.1039/x0xx00000x

View Article Online
DOI: 10.1039/C8DT04689A

valent metals. These findings have been also extended to N–H bonds in amides,[19,20] imidazoles, [21] imidazolines[22] and, in the context of ammonia fixation, to amines.[23] Although N–H bonds in amides have intrinsic very high BDE values (~95-110 kcal mol^{-1}; $BDFE_{calc.}$ ~93-108 kcal mol^{-1})[24] the corresponding reactivity and theoretical calculations suggest a considerable decrease of the BDFE by 34.5 and 66.8 kcal mol^{-1} after coordination with Ti(III)[19a] or Sm(II),[20] respectively. Remarkably, no experimental BDFE values for metal coordinated amides have been reported so far.

Within this context, the understanding of how to modify the reactivity of a M^n/M^{n+1} couple for hydrogen-atom transfer reactions can allow the system to work as a reductant (BDFE values lower than usual in C–H bonds) or an oxidant (BDFE higher than those described for C–H bonds), depending on the BDFE values of coordinated OH/NH ligands. Although some values for the BDFEs of different O–H bonds coordinated to diverse metals are known,[1,25] a large amount of basic investigation still remains to be done. Thus for example, the reported BDFE values are in many cases incomparable due to the influence of different aspects such as solvent effect, coordination issues or reversibility in the electrochemical measurement which can affect the value.[25d] Moreover, some contradicting works, mainly related with the functioning of lipoxygenases, have also been published.[26,27] Such intriguing case is related to a polypyridyl Fe(II) aquacomplex, which showed a remarkable BDFE diminishing of 42 kcal mol^{-1}.[26b] It is worth noting that the use of the same polypyridyl based ligands is able to diminish the BDFE of methanol by only 19.4 kcal mol^{-1} and the reasons are not very clear.[28] An experimental difficulty is also the lability of the exogenous ligands (water and methanol) in solution, which precludes a complete and comparative analysis. As we commented before, experimental BDFE values for amides coordinated to metals are lacking.

In this work, we have designed and synthesized new ligands in which we can explore for the first time how to modify the BDFE of O–H/(CO)N–HR bonds of series of metal complexes with different kinds of H-atom transferring groups, using as model the couple Fe(II)/Fe(III) (Figure 2). In this case, the X–H bonds studied are not exogenous ligands which prevents their lability in solution. The significant modification of the heteroatom–H BDFE by coordination to Fe(II) can be potentially interesting compared with other common hydrogen atom donors[29] in terms of structural flexibility, simple preparation and introduction of chirality, especially in the case of amides via the pendant side chain. As the main results, we estimate that Fe(II) complexes are able of weakening the coordinated X–H bonds by 10 to 26 kcal mol^{-1} depending on the nature of the ligands, and could be potentially used as hydrogen-atom donor (BDFE as low as 76 kcal mol^{-1}).

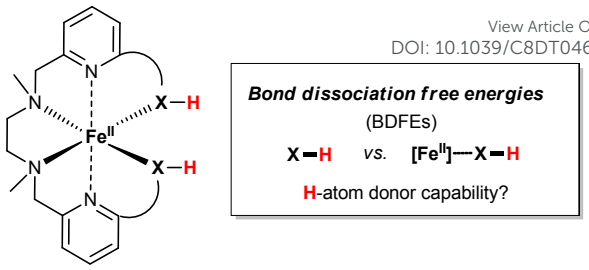

Figure 2. Working hypothesis

Results and discussion

We based our study on the previously described mep ligand (**1**) (mep = *N,N'*-dimethyl-*N,N'*-bis(2-pyridylmethyl)-ethane-1,2-diamine)[30] and functionalized derivatives mep(OH) (**2**), $mep(OH)_2$ (**3**), $mep(CONHBu)_2$ (**4**) (see ESI) and the corresponding Fe(II) complexes **5** to **8** (Figure 3). Those ligands possess pendant hydroxyl and amide groups covalently linked in the ligand framework, thus preventing their lability in solution. Therefore, the resulting complexes could be studied in aprotic solvents such as DMSO, in which the binding equilibrium of the ligand containing the desired hydrogen atom transferring group is simpler than in protic solvents. In this way, one or two benzylic alcohols/butyl amides remain coordinated to the metal, thus avoiding any intermolecular binding equilibrium measurements. Moreover, we can carry out the analysis of all the structures in the same aprotic solvent (DMSO), thus being consistent and comparable. Known ligand **1** was used to prepare the corresponding non-functionalized model complex **5** with neither hydroxy nor amide groups. We firstly synthetized ligands **1** to **4** from *N,N'*-dimethylethylenediamine (see ESI for details). Addition of $FeCl_2$ to the corresponding ligand solution in CH_3CN gave rise to complexes **5** to **8** that were firstly characterized by mass spectrometry (HRMS) (see ESI for details).

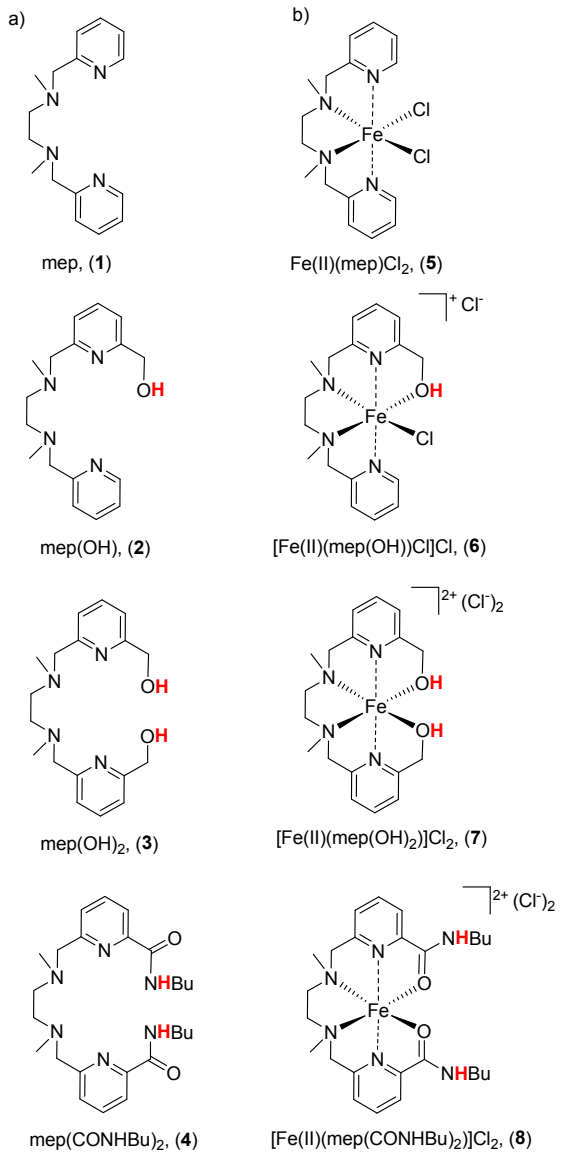

Figure 3. Ligands (**1**-**4**) and iron complexes (**5**-**8**) synthetized and studied.

X-Ray structures of complexes 6-8. Metal center coordination of the pendant groups is mandatory in this study. Remarkably, we could obtain the X-ray crystal structure of [Fe(II)(mep(OH))Cl]Cl (**6**), [Fe(II)(mep(OH)$_2$)]Cl$_2$ (**7**), and [Fe(II)(mep(CONHBu)$_2$)]Cl$_2$ (**8**) complexes, showing in all cases that in solid state the hydroxyl/carbonyl groups are coordinated to the Fe(II) center displacing even the negatively charged chloride counteranion, being an ideal situation to measure the BDFE of coordinated OH/(CO)NHBu groups (Figure 4). The preferred arrangement of the nitrogen ligands in all cases leaves two mutually *cis* coordination sites that are occupied by oxygen atoms. Uncoordinated chloride anions are located near the O–H bonds presumably interacting with them.

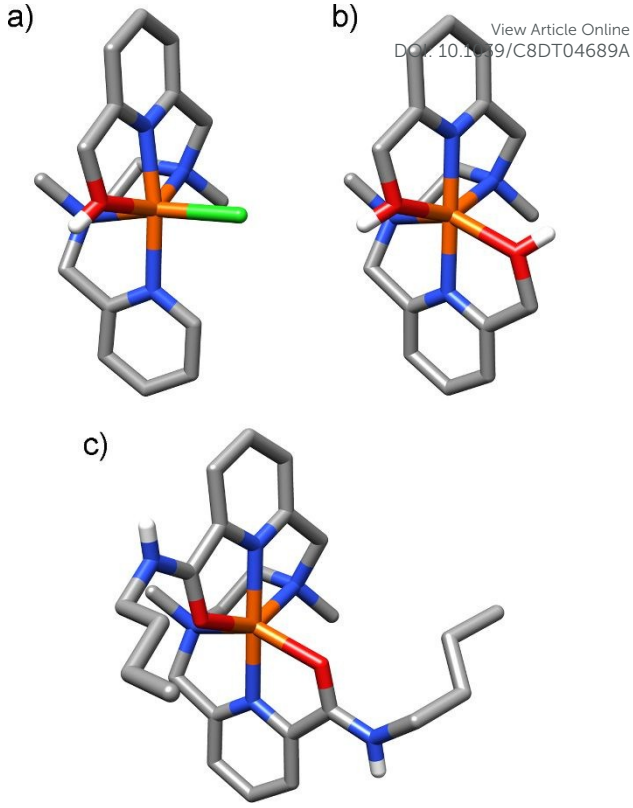

Figure 4. X-Ray crystal structures of: a) **6**, b) **7** and c) **8**. Color code: C: gray, O: red, N: blue, Fe: orange, Cl: green. H-atoms attached to carbon have been omitted for clarity.

NMR and EPR studies for complexes 6-8. Although these X-ray structures already show the tendency of OH/(CO)NHBu groups to coordinate to the metal center, a confirmation that this coordination is maintained in solution is also required. Therefore, we carried out the corresponding NMR studies in different solvents using also Fe(II)(mep)Cl$_2$ (**5**), as model compound. Although they are paramagnetic d^6 species we could obtain the corresponding ^{1}H-NMR spectra with signals spanning from –40 to 160 ppm.

Regarding the ^{1}H-NMR spectrum of model compound Fe(II)(mep)Cl$_2$ (**5**), it showed nine identifiable signals in CD_2Cl_2 (See ESI, Fig. S1), corresponding to the expected ones.[31,32]

We then analysed the behaviour of target complexes in solution. In the case of complex **6**, twelve identifiable signals can be clearly observed in the ^{1}H-NMR spectrum both in CD_2Cl_2 and DMSO-d_6 (See ESI, Figs. S3-S4). When we used other coordinating solvents such as CD_3OD or D_2O, a similar pattern could be also observed (See ESI, Figs. S5-S6). ^{1}H-NMR spectra of complex **7** in DMSO-d_6 and CD_3OD are, as expected, in agreement with a symmetric structure. In any case, the presence of a fast equilibrium between different metal-ligand configurations cannot be strictly excluded. The ^{1}H-NMR of complex **8**, [Fe(II)(mep(CONHBu)$_2$)]Cl$_2$ showed a similar set of signals using different solvents (CD_3OD, CD_3CN, CD_2Cl_2 and DMSO-d_6) ranging from 140 to –20 ppm, thus suggesting a similar structure in solution (See ESI, Figs. S9-S12). Coordination of amide group in all cases is then expected.

Complexes **6**-**8** are EPR silent when X-band measurements are carried out on grounded crystals, in good agreement with the

expected behaviour for iron systems with high spin (hs) +2 oxidation state (S = 2) and the paramagnetism shown in the NMR spectra. As a non-Kramer ion, Fe(II) usually results in short spin-lattice relaxation times and large zero-field splittings, causing the absence of EPR signals under normal experimental conditions.[33]

The thermal evolution of the magnetic susceptibility shows similar trends for complexes **6** to **8** (Figure 5, in which only the results for **8** are displayed, is illustrative of the behaviour of the three compounds). The χ_m curve increases continuously with decreasing temperature and no relative maximum is observed. The Curie-Weiss law is obeyed down to 50 K (See ESI, Figs. S16, S17) with values of the Curie constants (C_m, 6, 3.18; 7, 3.26; 8, 3.31 cm^3 K mol^{-1}) in the range usually found for *hs* Fe(II) compounds and small Weiss temperatures (θ, 6, –0.6; 7, –1.8; 8, –1.9 K). The room temperature χ_mT values (6, 3.17; 7, 3.23; 8, 3.28 cm^3 K mol^{-1}) are slightly larger than the spin-only value (3.00 cm^3 K mol^{-1}) predicted for S = 2 complexes due to spin-orbit coupling. For the three compounds, the χ_mT product remains roughly constant in the high temperature range (300-50 K), then decreases abruptly down to 5 K. This behaviour is characteristic of systems with antiferromagnetic interactions, but in these cases it is probably due to the zero-field splitting of the Fe(II) ions.[34] On the basis of this consideration, the experimental magnetic susceptibility data were fit to the following analytical expression,[35] which describes the thermal evolution of χ_m for an S = 2 ion undergoing zero-field splitting:

$$\chi_m = \frac{2Ng^2\mu_B^2}{3k(T-\theta)}\left[\frac{e^{-x}+4e^{-4x}+\frac{6}{x}(1-e^{-x})+\frac{4}{3x}(e^{-x}-e^{-4x})}{1+2e^{-x}+2e^{-4x}}\right] \quad \text{(eq. 1)}$$

where N, μ_B and k have their usual meaning, x = D/kT, D is the axial single-ion ZFS parameter, g is the average g factor and θ is the Weiss constant. The best least-squares fits (solid lines in Figs. 5, S16 and S17) were obtained for the ZFS parameters |D|/k= 10.6, 7.3 and 9.7 K with g = 2.06, 2.08 and 2.09 for compounds **6** to **8**, respectively. The θ values were fixed at those determined from the plots of χ_m^{-1} vs T. The calculated |D| values are similar to those usually observed for hs Fe(II) complexes and are high enough to explain the absence of X-band EPR signals.[36]

Isothermal magnetization data for compound **8** were collected in a field up to 7 T at various temperatures between 2 and 7 K. Deviations of the experimental data points from a Brillouin functions taken at the H/T values of the measurements is remarkable (inset of Fig. 5) and confirm the large ZFS of Fe(II) in this compound. Moreover, magnetization plot exhibits significant separation between the isofield curves (see Fig. S18 in ESI), indicative of strong magnetic anisotropy in the ground state. The high-field magnetization saturates at 2.41 BM, lower than the 4 BM expected for an isotropic system with four unpaired electrons and g = 2, but consistent with significant axial anisotropy.[37]

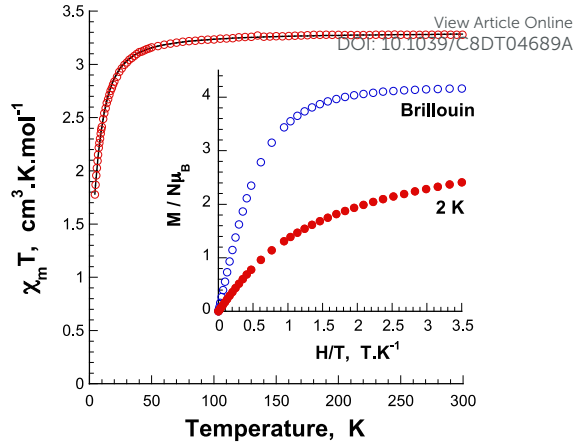

Figure 5. Temperature dependence of χmT for **8** measured at 0.1 T. The best fit to the data is shown as a solid line (see text for details of the fitting procedure). Inset: Field dependence of the magnetization for **8** measured at 2 K. The Brillouin function for S = 2 is shown for the sake of comparison.

BDFE values. Having synthesized and characterized all target compounds and once we confirmed that the OH/(CO)NHBu group remains coordinated in NMR scale to the metal center in complexes **6** to **8**, we proceeded to measure each homolytic bond dissociation free energy. BDFEs can be experimentally estimated by combining their pK_a values with the oxidation potentials of their conjugate bases both estimated in DMSO, according to the Bordwell´s methodology based on a thermodynamic cycle following equation 2 (Figure 6).[1,38] The constant C_G corresponds to the $H^{+/\cdot}$ standard reduction potential in the solvent of choice. We selected the revised value of C_G = 71.1 reported by Mayer *et al*. for DMSO using the redox potential referenced to $Fc^{+/0}$.[1]

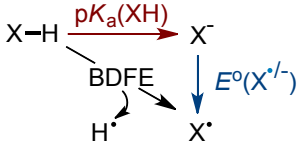

$$\mathbf{BDFE_{OH/CONRH}} = 1.37\ pK_a(OH/CONRH) + 23.06\ E^o(O^{\cdot-}/N^-) + C_G \text{ kcal mol}^{-1} \quad \text{(eq. 2)}$$

Figure 6. Thermodynamic cycle and Bordwell´s equation (eq. 2) for hydrogen atom dissociation.

pK_a measurements. We firstly measured the pK_a values of ligands **2** to **4** by UV-Vis titration in DMSO (See ESI, Figs. S19-21) using triphenylmethane anion (TH) as indicator (pK_a = 30.6).[39] Thus, we obtained the corresponding pK_a values (**2**, 27.6, **3**, 28.3/29.4, **4**, 22.0), being in agreement with previous reported data for benzylic alcohols (pK_a = 26.93-26.71),[40] and benzamides (23.5).[24a] In the case of **4** we determined only one pK_a value, thus suggesting that both deprotonation reactions exhibit similar pK_a values.

Comparison of the measured pK_a values for free ligands **1** to **4** with the values for the corresponding complexes **6** to **8** is useful to determine the influence of the Lewis acidity of the metal in the proton transfer from the ligand.

We then proceeded to measure the corresponding pK_a values for complexes **6** to **8** in DMSO (See ESI, Figs. S22-S24), which are

indispensable in the BDFE determination. We determined a pK_a value of 26.5 for [Fe(II)(mep(OH))Cl]Cl **6** in DMSO by UV-vis titration using triphenylmethane anion (TH) as indicator. This small variation with respect to free ligand **2** pK_a value (27.6) may be due to the low Lewis acidity of Fe(II) cation, that is very diminished in this monocationic complex by the presence of four donor nitrogenated ligands. Nevertheless, we cannot exclude either a fast equilibrium between coordinated and uncoordinated species in solution in the presence of coordinating chloride anion.[41] The only precedent, measured in DMSO, for a O–H bond coordinated to Fe(II) using a closely related ligand showed a striking pK_a value of only 8.1.[26b] It is worth noting that, in DMSO, the pK_a values for water and benzenesulphonic acid are 30 and 7, respectively, and therefore we do not have any plausible explanation for such extremely low value previously reported.

Complex [Fe(II)(mep(OH)$_2$)]Cl$_2$ **7** showed a pK_a of 23.8, being more acidic than the free ligand **3** (pK_a value around 28). This result is consistent with the existence of a much more rigid dicationic complex in solution in which both hydroxyl groups remain coordinated to the metal center.[42] Nevertheless, we could not discriminate between the two expected pK_a values.

The pK_a values for coordinated (CO)N–H bonds in [Fe(II)(mep(CONHBu)$_2$)]Cl$_2$ **8** were also estimated by UV-vis titrations using again red triphenylmethane anion as indicator, showing a pK_a value of only 19.7. This value is slightly more acidic that the estimated for the uncoordinated ligand **4** (22.0). Again, we could not discriminate between the two sequential deprotonation reactions.

Electrochemical properties. First of all we tried to evaluate the electrochemical features of ligands **1** to **4**. Unfortunately, we could not obtain the required E^0 values for deprotonated ligands by cyclic voltammetry measurements owing to the presence of adsorption peaks probably derived from decomposition reactions in the presence of base.[43] We assume that the BDFE of O–H/N–H bonds in our ligands are similar to those reported for benzyl alcohol (BDFE = 101.7 kcal mol^{-1})[40] and benzamide (BDE = 107 kcal mol^{-1}; BDFE$_{calc.}$ = 102.6 kcal mol^{-1}).[24a] In the case of benzyl alcohol, there are not many reported data for parent compounds owing to the benzylic C–H bond has a lower BDE value (79 kcal mol^{-1}) than the O–H bond. In that situation, the abstraction of H-atom from the benzylic C–H position is kinetically favoured with respect to the O–H bond, which may add a difficulty in the determination of BDE of O–H bond by other common methods based on H-abstraction reactivity. For benzamide, its reported BDE value is the same that the one reported for acetamide (BDE = 107 kcal mol^{-1}),[24a] suggesting that the nature of the substituent might not have an impact in the bond dissociation energy of N–H bond of the amide group. In this sense, although this assumption is reasonable, it makes the real decrease of the corresponding BDFE values after coordination with Fe(II) an estimation.

In the case of model complex (Fe(II)(mep)Cl$_2$) **5** in DMSO, cyclic voltammetry measurements showed two reversible oxidation peaks at –0.21 and –0.03 V vs Fc/Fc$^+$ (see ESI, Figure S27).[31,44] The relative intensity of these peaks changes depending on the sweep rate, suggesting the existence of two different structures in equilibrium in the homogeneous phase. To shed light about the nature of these species we carried out the corresponding cyclic voltammetry (CV) studies of model complex after counteranion chloride-SbF_6 exchange (see ESI, Figure S28). In this case, chloride anion coordination can be ruled out. Although the electrochemistry was more complex owing to adsorption processes in the electrode, two peaks were again observed, which could be attributed to a fast equilibrium between complexes presenting the pyridyl groups in *trans* and *cis* configurations.

CV of [Fe(II)(mep(OH))Cl]Cl **6** showed reversible oxidation peaks at –0.35 and –0.06 V, which could be attributable to a similar equilibrium process (Figure 7). In the presence of 1 equiv. of base (dimsyl anion, pK_a (DMSO) = 35.1)[39] these two peaks almost disappeared and a clear new reversible oxidation peak at –0.73 V (Fc/Fc$^+$) is detected. This value is similar to other Fe(II) alkoxides with similar chemical environment.[45] A peak at a very similar voltage can be also detected before the base addition, probably owing to a partial deprotonation in solution. The difference in the reduction potential in the presence and absence of base is expected as the addition of base generates a permanent donor alkoxide ligand.

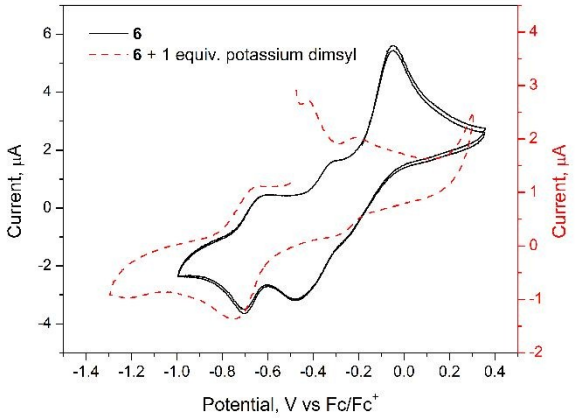

Figure 7. Cyclic voltammograms of **6** (4 mM) in DMSO in the absence and in the presence of potassium dimsyl (internal standard Fc/Fc$^+$, v = 0.1 V s^{-1}).

CV measurement of [Fe(II)(mep(OH)$_2$)]Cl$_2$ **7** in DMSO showed peaks at –0.36 and –0.03 V, in the same range as those obtained for [Fe(II)(mepOH)Cl]Cl **6**, considering also the uncertainties associated to the irreversibility of the process. In the presence of an excess of base (dimsyl anion) a clear reversible peak can be detected at –1.2 V (Figure 8). This shift of the oxidation potential towards more negative values is also consistent with a Fe(II) complex with two donating alkoxide groups after the addition of base. Remarkably, in the presence of only one equivalent of base, other reversible peaks at –0.78 V was observed which can be attributed to the mono-deprotonated complex. In fact, such E^0 value is similar to that previously obtained for **6** in the presence of base (–0.73 V). As in the case of complex **6**, peaks at a very similar voltage can be also detected before the base addition, resulting of partial deprotonating events in solution.

View Article Online
DOI: 10.1039/C8DT04689A

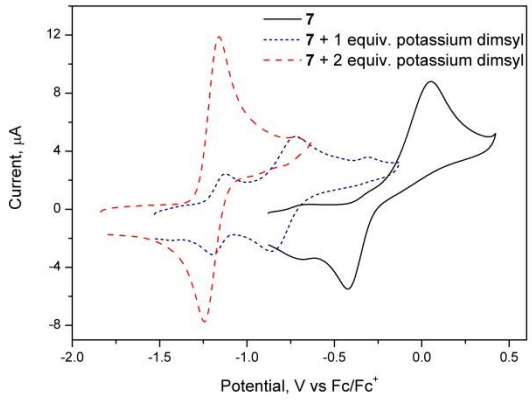

Figure 8. Cyclic voltammograms of **7** (4 mM) in DMSO in the absence and in the presence of potassium dimsyl (internal standard Fc/Fc^+, v = 0.1 V s^{-1}).

In the case of $[Fe(II)(mep(CONHBu)_2)]Cl_2$ **8** in DMSO, the CV showed a complex situation but a reversible peak at –0.38 V could be assigned to the Fe(II)/Fe(III) pair (Figure 9). In the presence of an excess of base, a clear and reversible peak was detected at –0.76 V corresponding to the fully deprotonated complex. Moreover, clear reversible reduction peaks for **8** were also observed in the absence (–1.87 V) and presence (–2.39 V) of base, which are associated with Fe(II)/Fe(I) pair. Unfortunately, in this case no clear peaks attributed to the monodeprotonating process could be observed.

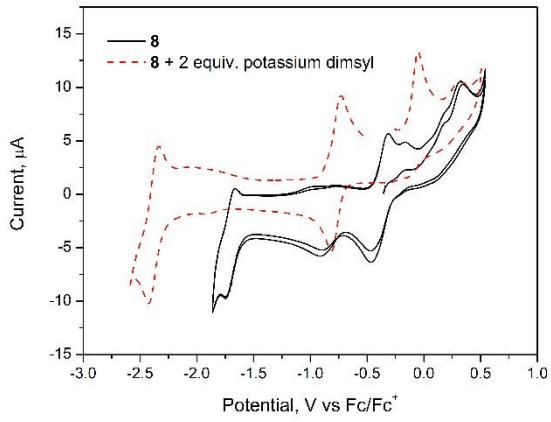

Figure 9. Cyclic voltammograms of **8** (4 mM) in DMSO in the absence and in the presence of potassium dimsyl (internal standard Fc/Fc^+, v = 0.1 V s^{-1}).

BDFE estimation. Following equation 2 (Figure 6), we estimated a BDFE value for [Fe(II)(mep(OH))Cl]Cl **6** of 90.5 kcal mol^{-1}, which represents an estimated BDFE weakening of around 10 kcal mol^{-1} by coordination to the metal center (Figure 10a). In the case of $[Fe(II)(mep(OH)_2)]Cl_2$ **7** an estimation of the BDFE for the first and second hydroxyl group could be obtained (Figure 10b). The BDFE value for the first coordinated OH group (pK_a = 23.8, E^0 = –0.78 V *vs* Fc/Fc^+) is 85.7 kcal mol^{-1}, which is consistent with the value obtained for [Fe(II)(mep(OH))Cl]Cl **6**. The BDFE of the second hydroxyl group of complex **7** is diminished to only 76.0 kcal mol^{-1} (pK_a = 23.8, E^0 = –1.2 V *vs* Fc/Fc^+), which is again consistent with an increase of the electron density in the metal center by the existence of a new alkoxide ligand. This BDFE value is similar to that recently reported for a Fe(II) aquacomplexes (68.6 and 84 kcal mol^{-1})[26c,26d] and represents an estimated weakening of about 26 kcal mol^{-1} by coordination to a Fe(II) center. The resulting value of just 76.0 kcal mol^{-1} is in the range of other common hydrogen atom donors such as 1,4-ciclohexadiene (BDE = 76 kcal mol^{-1}; BDFE = 67.8 kcal mol^{-1}).[1]

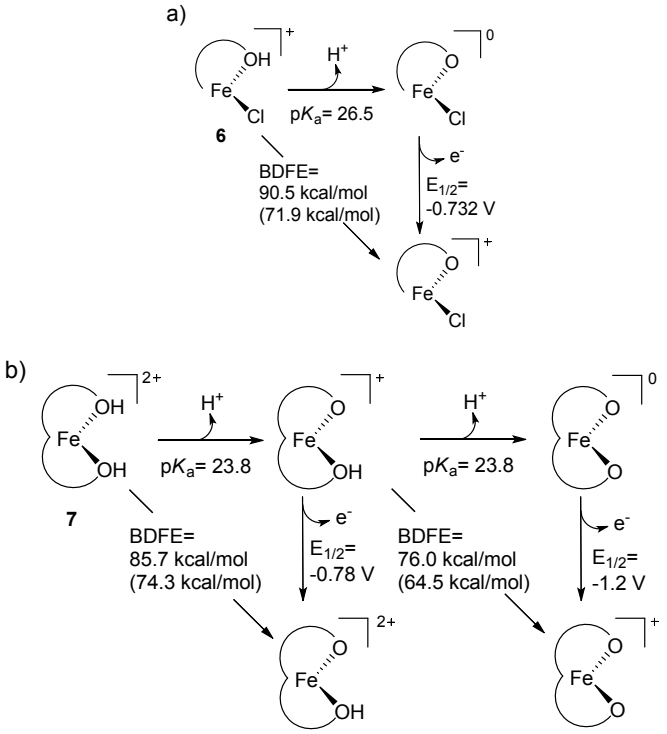

Figure 10. Thermodynamic cycle for a) [Fe(II)(mep(OH))Cl]Cl, **6** and b) $[Fe(II)(mep(OH)_2)]Cl_2$, **7** developed in DMSO to evaluate the BDE(O–H) with redox potentials referenced to the Fc/Fc^+ couple (DFT-calculated theoretical BDFE values shown in brackets).

DFT-based theoretical calculations (Gaussian09, B3LYP/6-31G(d,p)) are in qualitative agreement with all these findings (Table 1). Thus, coordination of the hydroxyl group with Fe(II) promotes a calculated diminishing in BDFE of 17.7 and 16.3 kcal mol^{-1} for complexes [Fe(II)(mep(OH))dmso] and $Fe(II)(mep(OH)_2)$, respectively, as optimized model compounds for **6** and **7**. In the case of the BDFE associated to the second hydroxyl group of $Fe(II)(mep(OH)_2)$ a subsequent decrease of 9.8 kcal mol^{-1} was also theoretically estimated, which is in reasonable agreement with the experimentally observed trend.

Table 1. Calculated BDFE values for the systems studied

Complex	BDFE [kcal/mol]
mep(OH), (**2**)	89.6
mep(OH)$_2$, (**3**)	90.9
mep(CONHBu)$_2$, (**4**)	93.7
Fe(II)(mep(OH))(dmso), (as model of **6**)	71.9
Fe(II)(mep(OH)$_2$), (as model of **7**)	74.3 (1st) 64.5 (2nd)
Fe(II)(mep(CONHBu)$_2$), (as model of **8**)	90.6 (1st) 80.6 (2nd)

With the experimental data obtained the BDFE value for the second coordinated (CO)NH group (pK_a =19.7, E^0 = –0.76 V *vs* Fc/Fc$^+$) resulted in 80.5 kcal mol^{-1}. This decrease is less pronounced than in the case of OH group probably because the negative charge is stabilized by the carbonyl group, thus having less influence in the electronic structure of the metal. In any case, the coordination with Fe(II) promotes a decrease of the BDFE of N–H bonds in the amide as it has been previously suggested. Again, theoretical calculations qualitatively support these findings (*ca.* 3 and 13 kcal mol^{-1} diminishing, respectively).

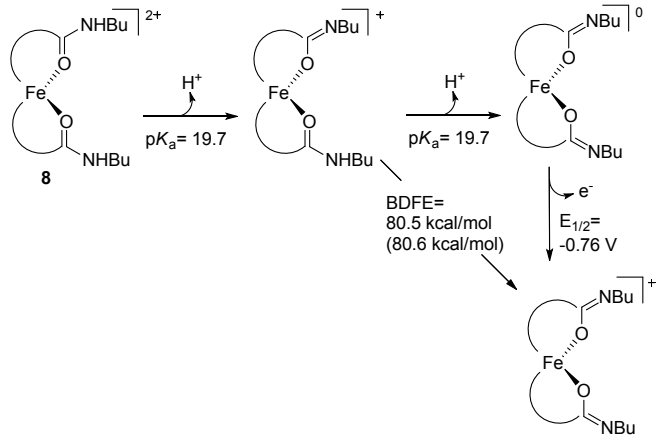

Figure 11. Thermodynamic cycle for [Fe(II)(mep(CONHBu$_2$)]Cl$_2$, **8** developed in DMSO to evaluate the BDE((CO)N–HBu) with redox potentials referenced to the Fc/Fc$^+$ couple (DFT-calculated theoretical BDFE values shown in brackets).

Conclusions

In conclusion, we have shown that new ligands **2** to **4** are interesting scaffolds to measure the BDFE values of hydroxyl and carbamoyl groups interacting with a Fe(II) metallic center. This study can be extended to other metals in order to evaluate their properties as hydrogen-atom donors in a consistent way. The presented results also show that, in certain chemical environments, hydroxyl and amides groups coordinated to Fe(II) can be transformed into reasonable hydrogen-atom donors (BDFEs of 76.0 and 80.5 respectively). It is worth noting that these kinds of BDFE values are scarce, especially in the case of iron complexes. Amides are especially attractive as they could bear chiral information and work in that direction is now underway.

Experimental section

General Section. All reagents and solvents (CH_2Cl_2, EtOAc, hexane, CH_3CN, CH_3OH) were purchased from standard chemical suppliers and used without further purification. Anhydrous solvents (CH_3OH, CH_2Cl_2, CH_3CN and DMSO) were purchased from standard suppliers. Thin-layer chromatography analysis was performed on aluminium-backed plates coated with silica gel 60 (230-240 mesh) with F_{254} indicator. The spots were visualized with UV light (254 nm) and/or stained with phosphomolybdic acid (10% ethanol solution) and subsequent heating. Chromatography purifications were performed with silica gel 60 (40-63 μm) or with neutral aluminium oxide (50-200 μm). ^{1}H NMR spectra were recorded on Varian 300, 400 or 500 MHz spectrometers, at a constant temperature of 298 K. Chemical shifts are reported in ppm using residual solvent peak as reference ($CHCl_3$: δ = 7.26 ppm, CH_3OH: δ = 3.31 ppm, CH_3CN: δ = 1.94 ppm, DMSO: δ = 2.50 ppm, CH_2Cl_2: δ = 5.32 ppm). Data are reported as follows: chemical shift, multiplicity (s: singlet, d: doublet, t: triplet, q: quartet, quint: quintuplet, hept: heptuplet, m: multiplet, dd: doublet of doublets, dt: doublet of triplets, td: triplet of doublets, bs: broad singlet), coupling constant (*J* in Hz) and integration; ^{13}C NMR spectra were recorded at 75, 101 or 126 MHz using broadband proton decoupling and chemical shifts are reported in ppm using residual solvent peaks as reference ($CHCl_3$: δ = 77.16 ppm, CH_3OH: δ = 49.00 ppm). Carbon multiplicities were assigned by DEPT techniques. High-resolution mass spectra (HRMS) were recorded using EI at 70eV on a Micromass AutoSpec (Waters) or by ESI mass spectrometry carried out on a QSTAR ABSciex mass spectrometer. Ligand **1** was known and the obtained ^{1}H- and ^{13}C-NMR data matched with those previously described.[46]

Ligand characterization:

mep(OH) (**2**). Brownish syrup; **^{1}H NMR (500 MHz, $CDCl_3$):** δ 8.51 (ddd, *J* = 4.9, 1.8, 0.9 Hz, 1H), 7.62 (td, *J* = 7.8, 1.8 Hz, 1H), 7.60 (t, *J* = 7.6 Hz, 1H), 7.41 (d, *J* = 7.9 Hz, 1H), 7.29 (d, *J* = 7.6 Hz, 1H), 7.13 (ddd, *J* = 7.6, 4.9, 1.2 Hz, 1H), 7.10 (d, *J* = 7.7 Hz, 1H), 4.72 (s, 2H), 3.69 (s, 4H), 2.64 (s, 4H), 2.27 (s, 6H). **^{13}C NMR (126 MHz, $CDCl_3$):** δ 159.3 (C), 158.6 (C), 158.3 (C), 149.2 (CH), 137.2 (CH), 136.6 (CH), 123.3 (CH), 122.1 (CH), 121.7 (CH), 118.9 (CH), 64.2 (CH_2), 63.9 (CH_2), 55.5 (CH_2), 55.4 (CH_2), 43.0 (CH_3), 43.0 (CH_3). **HRMS (ESI):** *m/z* [M+H]$^+$ calcd for $C_{17}H_{25}N_4O$: 301.2022; found: 301.2014. **IR (ATR):** 3280, 2920, 2846, 2800, 1660, 1593, 1576, 1455, 1436, 1358, 1070, 1033, 760 cm^{-1}.

mep(OH)$_2$ (**3**). Brownish syrup; **^{1}H NMR (500 MHz, MeOD):** δ 7.77 (t, *J* = 7.7 Hz, 2H), 7.41 (d, *J* = 7.8 Hz, 2H), 7.36 (d, *J* = 7.8 Hz, 2H), 4.67 (s, 4H), 3.66 (s, 4H), 2.63 (s, 4H), 2.26 (s, 6H). **^{13}C NMR (126 MHz, MeOD):** δ 161.8 (C), 159.1 (C), 138.9 (CH), 123.2 (CH), 120.3 (CH), 65.5 (CH_2), 64.4 (CH_2), 56.0 (CH_2), 43.2 (CH_3). **HRMS (ESI):** *m/z* [M+H]$^+$ calcd for $C_{18}H_{27}N_4O_2$: 331.2129; found: 331.2130. **IR (ATR):** 3197, 2846, 2814, 1595, 1576, 1441, 1357, 1092, 1072, 1040, 999, 969, 783, 618 cm^{-1}.

mep(CONHBu)$_2$ (**4**). Brownish solid; **^{1}H NMR (500 MHz, $CDCl_3$):** δ 8.15 (s, 2H), 8.08 (dd, *J* = 7.7, 1.1 Hz, 2H), 7.78 (t, *J* = 7.7 Hz,

2H), 7.54 (dd, *J* = 7.7, 1.1 Hz, 2H), 3.72 (s, 4H), 3.46 (q, *J* = 6.8 Hz, 4H), 2.64 (s, 4H), 2.29 (s, 6H), 1.62 (p, *J* = 7.6 Hz, 4H), 1.42 (h, *J* = 7.3 Hz, 4H), 0.96 (t, *J* = 7.4 Hz, 6H). **^{13}C NMR (126 MHz, $CDCl_3$):** δ 164.3 (C), 158.0 (C), 149.4 (C), 137.6 (CH), 125.3 (CH), 120.6 (CH), 63.9 (CH_2), 55.4 (CH_2), 42.9 (CH_3), 39.1 (CH_2), 31.8 (CH_2), 20.2 (CH_2), 13.8 (CH_3). **HRMS (ESI):** *m/z* $[M]^+$ calcd for $C_{26}H_{41}N_6O_2$: 469.3285; found: 469.3286. **IR (ATR):** 3308, 2952, 2929, 2804, 1657, 1526, 1453, 712 cm^{-1}.

Synthesis of the Complexes 5-8. $FeCl_2{\cdot}4H_2O$ (1 equiv.) was added to a CH_3CN (0.3 M) solution of the corresponding ligand (1 equiv.) and the mixture stirred at room temperature for 16 h under Ar atmosphere. Then Et_2O was added and the slurry was stirred for 15 min. The solid was filtered using a sintered glass Buchner funnel with paper filter. The solid was washed with Et_2O several times, dried and collected. Samples constituted of single crystals were obtained by vapour diffusion using CH_3CN / CH_3OH or DMF as solvent and Et_2O as precipitant. All the measurements were carried out with single crystals to ensure unequivocal composition of the sample.

Fe(II)(mep)Cl_2 (5): 365 mg, 72% yield, yellow powder. After crystallization: brown crystals. **HRMS (ESI):** *m/z* $[M\text{-}Cl]^+$ calcd for $C_{16}H_{22}N_4ClFe$: 361.0876; found: 361.0868. **HRMS (ESI):** *m/z* $[M\text{-}Cl_2]^{2+}$ calcd for $C_{16}H_{22}N_4Fe$: 163.0591; found: 163.0591. **IR (ATR):** 2970, 1601, 1467, 1432, 1303, 1080, 1052, 1013, 978, 817, 777 cm^{-1}. **Elemental Analysis of single crystal:** Calcd for $C_{16}H_{22}N_4FeCl_2{\cdot}0.5H_2O$: C, 47.67; H, 5.41; N, 14.07; found: C, 47.32; H, 5.71; N, 13.80.

[Fe(II)(mep(OH))Cl]Cl (6): 142 mg, 98% yield, yellow powder. After crystallization: brown crystals; **HRMS (ESI):** *m/z* $[M\text{-}HCl]^+$ calcd for $C_{17}H_{23}N_4OClFe$: 390.0904; found: 390.0892. **IR (ATR):** 2815, 2714, 1580, 1605, 1443, 1039, 817, 769 cm^{-1}. **Elemental Analysis of single crystal:** Calcd for $C_{17}H_{24}N_4OFeCl_2{\cdot}0.5CH_3CN$: C, 48.29; H, 5.74; N, 14.08; found: C, 48.19; H, 5.61; N, 14.01.

[Fe(II)(mep($OH)_2$)]Cl_2 (7): 444 mg, 88% yield, yellow powder. After crystallization: bright yellow crystals. **HRMS (ESI):** *m/z* $[M\text{-}H_2Cl_2]^{2+}$ calcd for $C_{18}H_{24}N_4O_2Fe$: 192.0618; found: 192.0625. **IR (ATR):** 1604, 1579, 1419, 1029, 816, 770, 745 cm^{-1}. **Elemental Analysis of single crystal:** Calcd for $C_{18}H_{26}N_4O_2FeCl_2{\cdot}0.5H_2O$: C, 46.38; H, 5.84; N, 12.02; found: C, 46.29; H, 5.60; N, 11.99.

[Fe(II)(mep(CONHBu)$_2$)]Cl_2 (8): 346 mg, 81% yield, red powder. After crystallization: bright deep red crystals. **IR (ATR):** 2957, 2864, 1626, 1599, 1549, 1465, 826, 767, 532 cm^{-1}. **HRMS (ESI):** *m/z* $[M\text{-}HCl_2]^+$ calcd for $C_{26}H_{39}N_6O_2Fe$: 523.2478; found: 523.2464; *m/z* $[M\text{-}Cl_2]^{2+}$ calcd for $C_{26}H_{40}N_6O_2Fe$: 262.1275; found: 262.1280. A good elemental analysis for the corresponding single crystal could not be obtained.

Single-crystal X-ray Diffraction. The X-ray diffraction data were collected on a Bruker D8 Venture diffractometer equipped with a Photon 100 detector using Mo or Cu radiation sources or a Bruker Smart APEX diffractometer with an APEX detector using a Mo radiation source. The structures were solved with SHELXT[47] and refined using the full-matrix least-squares against F^2 procedure with SHELX 2016[48] using the WinGX32[49] software.

Physical Measurements: X-band EPR measurements were carried out on a Bruker ELEXSYS 500 spectrometer equipped with a super-high-Q resonator ER-4123-SHQ, a maximum available microwave power of 200 mW and standard Oxford Instruments low temperature devices. Samples were placed in quartz tubes and spectra were recorded at different temperatures between 5 and 300 K. The magnetic field was calibrated by a NMR probe and the frequency inside the cavity (~9.4 GHz) was determined with an integrated MW-frequency counter. Variable temperature (5-300 K) magnetic susceptibility measurements on polycrystalline samples were carried out with a Quantum Design MPMS3 SQUID magnetometer under a magnetic field of 0.1 T. The experimental susceptibilities were corrected for the diamagnetism of the constituent atoms by using Pascal's constants. Magnetization as a function of applied field (H) was measured using the same magnetometer at several temperatures below 10 K after cooling the samples in zero- field. During the measurement, the field was swept between 0 and 7 T.

Measurement of pK_a values. pK_a measurements were carried out on a Specord 200 Plus Analytik Jena UV-Visible spectrophotometer by UV-vis titration using triphenylmethane anion as indicator.

Preparation of potassium dimsyl solution. Under argon atmosphere, KH in mineral oil was washed with several portions of dry hexane. Then, KH (50 mg) was dissolved in dry DMSO (5 mL) and bubbles appeared immediately. The flask was wrapped with aluminum foil and stirred under argon until the bubbling ceased. The solution was kept under argon at 0°C and it was stable for 1 day.

Preparation of triphenylmethane anion solution. In a UV-vis cuvette and under Ar atmosphere, a 0.06 M solution of triphenylmethane (30 mg) in dry DMSO (2 mL) was prepared. Three or four drops of potassium dimsyl solution were added and solution turned red. Red color must be constant before starting the titration, keeping initial absorbance maximum at 499 nm around 1.0.

UV-vis titration. Aliquots of a 0.02 M solution of ligand/iron complex in dry DMSO were added to a triphenylmethane anion solution in DMSO and UV-vis spectra were recorded between 400-600 nm at 25 °C. (Final added volume did not exceed the 10% of initial volume in any case). Decrease of absorbance maximum at 499 nm were plot against concentration of ligand/iron complex.

Electrochemistry. Electrochemical measurements were carried out under Ar atmosphere at 25 °C using a PGSTST204 potentiostat galvanostat (Metrohm Autola B. V.) with a three-electrode cell in 0.1 M solution of tetra-*n*-butylammonium hexafluorophosphate ($TBAPF_6$) in DMSO as the supporting electrolyte. A glassy carbon disc was used as the working electrode, a platinum wire as the counterelectrode, and a silver wire as the quasi-reference electrode. The Pt-wire and Ag-wire were flamed to ensure the absence of impurities. Dry DMSO was used as solvent to prepare a 0.1 M solution of tetra-*n*-butylammonium hexafluorophosphate ($TBAPF_6$) which was used as work solution. All of the voltammograms were initiated from the null current potential and the scan was initiated in both the positive and the negative directions at a scan rate of 0.1 V/s. Potential values are referred to ferrocene/ferrocenium system (Fc/Fc^+), being ferrocene added as internal reference after each measurement. For the working conditions, the

electroactive domain was between –2.0 and 1.0 V *vs* Fc^+/Fc. CV measurements were recorded before and after the addition of excess of base (potassium dimsyl solution).

Calculation of experimental bond dissociation energies (BDE). The experimental homolytic bond dissociation of O–H and N–H bonds in the iron complexes were estimated by combining their pK_a values with the oxidation potentials of their conjugate bases according to Bordwell´s methodology, following eq. 2.

Theoretical calculations. DFT theoretical calculations were performed with Gaussian 09.[50] The calculations were carried out at the B3LYP/6-31G(d,p) level for C, H, N, O and S atoms, while the LanL2DZ effective core potential of Wadt and Hay and its basis set was used for Fe.[51] The calculations were done in DMSO using the polarizable continuum model with the integral equation formalism (IEFPCM) included in Gaussian 09.[52] Calculations of Fe(II)(mep($CONHBu)_2$) complexes were carried out using a ultra-fine integration grid. Frequency calculations were performed to confirm the optimized structures corresponded to an energy minimum. Bond dissociation free energy (BDFE) theoretical values were calculated as the difference between the free energy of the deprotonated or doubly deprotonated Fe(III) complexes and the sum of the free energies of the starting Fe(II) complexes and a H atom, calculated independently. The value of the sum of electronic and thermal free energies was used. High spin systems were considered for both Fe(II) and Fe(III) complexes. Counterions were not included in the calculations. A BDFE value in better agreement with the experimental one was obtained for the Fe(II)(mep(OH)) system if the coordinated Cl atom was replaced by a DMSO molecule.

Conflicts of interest

There are no conflicts to declare.

Acknowledgements

We thank the Ministerio de Economía y Competitividad (MINECO, Spain) (CTQ2014-53598-R) and Junta de Andalucía (FQM2012-790). S.R. thanks the MECD for FPU predoctoral fellowship. A.M. and A.G.C. thank the MINECO for IJCI-2016-27793 and RyC-2013-12943 contracts.

Notes and references

1 J. J. Warren, T. A. Tronic and J. M. Mayer, *Chem. Rev.*, 2010 **110**, 6961–7001.
2 (*a*) C. E. Elwell, N. L. Gagnon, B. D. Neisen, D. Dhar, A. D. Spaeth, G. M. Yee and W. B. Tolman, *Chem. Rev.,* 2017, **117**, 2059–2107; (*b*) Z. Chen and G. Yin, *Chem. Soc. Rev.*, 2015, **44**, 1083–1100.
3 (*a*) C. Krebs, S. Chen, J. Baldwin, B. A. Ley, U. Patel, D. E. Edmondson, B. H. Huynh and J. M. Bollinger, *J. Am. Chem. Soc.*, 2000, **122**, 12207–12219; (*b*) J. Baldwin, W. C. Voegtli, N. Khidekel, P. Moënne-Loccoz, C. Krebs, A. S. Pereira, B. A. Ley, B. H. Huynh, T. M. Loehr, P. J. Riggs-Gelasco, A. C. Rosenzweig and J. M. Bollinger, *J. Am. Chem. Soc.*, 2001, **123**, 7017–7030.
4 A. G. Campaña, E. Buñuel, J. M. Cuerva and D. J. Cárdenas, *Chem. Eur. J.,* 2013, **19**, 16187–16191.
5 E. Derat and S. Shaik, *J. Am. Chem. Soc.*, 2006, **128**, 13940–13949.
6 J. Stubbe, D. G. Nocera, C. S. Yee and M. C. Y. Chang, *Chem. Rev.*, 2003, **103**, 2167–2201.
7 N. Mitic, M. D. Clay, L. Saleh, J. M. Bollinger and E. I. Solomon, *J. Am. Chem. Soc.*, 2007, **129**, 9049–9065.
8 (*a*) K. Roos and P. E. M. Siegbahn, *Biochemistry*, 2009, **48**, 1878–1887; (*b*) W. Jiang, D. Yun, L. Saleh, E. W. Barr, G. Xing, L. M. Hoffart, M. A. Maslak, C. Krebs and J. M. Bollinger Jr., *Science*, 2007, **316**, 1188–1191; (*c*) N. Voevodskaya, F. Lendzian, A. Ehrenberg and A. Gräslund, *FEBS Lett.*, 2007, **581**, 3351–3355; (*d*) J. M. Bollinger Jr, W. Jiang, M. T. Green and C. Krebs, *Curr. Opin. Struct. Biol.*, 2008, **18**, 650–657.
9 C. S. Andersson and M. Högbom, *Proc. Nat. Acad. Sci*, 2009, **106**, 5633–5638.
10 (*a*) C. W. Hoganson and G. T. Babcock, *Science*, 1997, **277**, 1953–1956; (*b*) J. M. Keough, D. L. Jenson, A. N. Zuniga and B. A. Barry, *J. Am. Chem. Soc.*, 2011, **133**, 11084–11087; (*c*) H. Matsuoka, J.-R. Shen, A. Kawamori, K. Nishiyama, Y. Ohba, and S. Yamauchi, *J. Am. Chem. Soc.,* 2011, **133**, 4655–4660.
11 Y. Umena, K. Kawakami, J.-R. Shen and N. Kamiya, *Nature*, 2011, **473**, 55–60.
12 B. A. Barry, U. Brahmachari and Z. Guo, *Acc. Chem. Res.,* 2017, **50**, 1937–1945.
13 (*a*) M. T. Caudle and V. L. Pecoraro, *J. Am. Chem. Soc.,* 1997, **119**, 3415–3416; (*b*) M. J. Baldwin and V. L. Pecoraro, *J. Am. Chem. Soc.,* 1996, **118**, 11325–11326.
14 M. R. A. Blomberg, P. E. M. Siegbahn, S. Styring, G. T. Babcock, B. Åkermark and P. Korall, *J. Am. Chem. Soc.*, 1997, **119**, 8285–8292.
15 R. Gupta, C. E. MacBeth, V. G. Young Jr. and A. S. Borovik, *J. Am. Chem. Soc.,* 2002, **124**, 1136–1137.
16 (*a*) V. L. Pecoraro, M. J. Baldwin, M. T. Cudle, W.-Y. Hsieh and N. A. Law, *Pure Appl. Chem.*, 1998, **70**, 925–929; (*b*) R. J. Pace, R. Stranger and S. Petrie, *Dalton Trans.*, 2012, **41**, 7179–7189; (*c*) M. M. Najafpour, G. Renger, M Hołyńska, A. N. Moghaddam, E.-M. Aro, R. Carpentier, H. Nishihara, J. J. Eaton-Rye, J.-R. Shen and S. I. Allakhverdiev, *Chem. Rev.* 2016, **116**, 2886–2936.
17 (*a*) J. M. Cuerva, A. G. Campaña, J. Justicia, A. Rosales, J. L. Oller-López, R. Robles, D. J. Cárdenas, E. Buñuel and J. E. Oltra, *Angew. Chem. Int. Ed.,* 2006, **45**, 5522–5526; (*b*) T. Jiménez, A. G. Campaña, B. Bazdi, M. Paradas, D. Arráez-Román, A. Segura-Carretero, A. Fernández-Gutiérrez, J. E. Oltra, R. Robles, J. Justicia and J. M. Cuerva, *Eur. J. Org. Chem.,* 2010, 4288–4295; (*c*) M. Paradas, A. G. Campaña, T. Jiménez, R. Robles, J. E. Oltra, E. Buñuel, J. Justicia, D. J. Cárdenas and J. M. Cuerva, *J. Am. Chem. Soc.,* 2010, **132**, 12748–12756; (*d*) M. Paradas, A. G. Campaña, M. L. Marcos, J. Justicia, A. Haidour, R. Robles, D. J. Cárdenas, J. E Oltra and J. M. Cuerva, *Dalton Trans.,* 2010, **39**, 8796–8800.
18 (*a*) T. V. Chciuk and R. A. Flowers II, *J. Am. Chem. Soc.,* 2015, **137**, 11526−11531; (*b*) T. V. Chciuk, W. R. Anderson Jr. and R. A. Flowers II, *Angew. Chem. Int. Ed.,* 2016, **55**, 6033–6036; (*c*) T. V. Chciuk, W. R. Anderson Jr. and R. A. Flowers II, *J. Am. Chem. Soc.*, 2016, **138**, 8738−8741; (*d*) T. V. Chciuk, W. R. Anderson, Jr. and R. A. Flowers II, *Organometallics*, 2017, **36**, 4579−4583; (*e*) S. S. Kolmar and J. M. Mayer, *J. Am. Chem. Soc.*, 2017, **139**, 10687−10692.
19 (a) Y.-Q. Zhang, V. Jakoby, K. Stainer, A. Schmer, S. Klare, M. Bauer, S. Grimme, J. M. Cuerva and A. Gansäuer, *Angew. Chem. Int. Ed.*, 2016, **55**, 1523–1526; (b) K. T. Tarantino, D. C. Miller, T. A. Callon and R. R. Knowles, *J. Am. Chem. Soc.*, 2015, **137**, 6440–6443.
20 T. V. Chciuk, A. M. Li, A. Vazquez-Lopez, W. R. Anderson Jr. and R. A. Flowers II, *Org. Lett.*, 2017, **19**, 290–293.

21 J. J. Warren and J. M. Mayer, *J. Am. Chem. Soc.*, 2008, **130**, 2774–2776.
22 J. P. Roth and J. M. Mayer, *Inorg. Chem.*, 1999, **38**, 2760–2761.
23 (*a*) I. Pappas and P. J. Chirik, *J. Am. Chem. Soc.*, 2015, **137**, 3498–3501; (*b*) I. Pappas and P. J. Chirik, *J. Am. Chem. Soc.*, 2016, **138**, 13379–13389; (*c*) M. J. Bezdek, S. Guo and P. J. Chirik, *Science*, 2016, **354**, 730–733; (*d*) G. W. Margulieux, M. J. Bezdek, Z. R. Turner and P. J. Chirik, *J. Am. Chem. Soc.,* 2017, **139**, 6110–6113.
24 In case of missing BDFE values, they have been recalculated using ref. 1: (*a*) F. G. Bordwell, J. A. Harrelson and T.-Y. Lynch, *J. Org. Chem.*, 1990, **55**, 3337–3341; (*b*) F. G. Bordwell and G.-Z. Ji, *J. Am. Chem. Soc.*, 1991, **113**, 8398–8401; (*c*) F. G. Bordwell, S. Zhang, X.-M. Zhang and W.-Z. Liu, *J. Am. Chem. Soc.,* 1995, **117**, 7092–7096; (*d*) J.-P. Cheng and Y. Zhao, *Tetrahedron*, 1993, **49**, 5267–5276; (*e*) J. R. B. Gomes, M. D. M. C. Ribeiro da Silva and M. A. V. Ribeiro da Silva, *J. Phys. Chem. A*, 2004, **108**, 2119–2130.
25 (*a*) N. Kindermann, C. J. Günes, S. Dechert and F. Meyer, *J. Am. Chem. Soc.,* 2017, **139**, 9831–9834; (*b*) G. Ali, P. E. VanNatta, D. A. Ramirez, K. M. Light and M. T. Kieber-Emmons, *J. Am. Chem. Soc.*, 2017, **139**, 18448–18451; (*c*) D. Dhar, G. M. Yee, A. D. Spaeth, D. W. Boyce, H. Zhang, B. Dereli, C. J. Cramer and W. B. Tolman, *J. Am. Chem. Soc.*, 2016, **138**, 356–368; (d) D. Dhar and W. B. Tolman, *J. Am. Chem. Soc.*, 2015, **137**, 1322–1329.
26 (*a*) C. R. Goldsmith, R. T. Jonas and T. D. P. Stack, *J. Am. Chem. Soc.,* 2002, **124**, 83–96; (*b*) C. R. Goldsmith and T. D. P. Stack, *Inorg. Chem.*, 2006, **45**, 6048–6055; (*c*) H. Gao and J. T. Groves, *J. Am. Chem. Soc.*, 2017, **139**, 3938–3941; (*d*) L. M. Brimes, M. K. Coggins, P. C. Y. Poon, S. Toledo, W. Kaminsky, M. L. Kirk and J. A. Kovacs, *J. Am. Chem. Soc.*, 2015, **137**, 2253–2264.
27 For BDE values on Fe(II)-hydroxides see: R. Gupta and A. S. Borovik, *J. Am. Chem. Soc.,* 2003, **125**, 13234–13242.
28 An extremely low pK_a value of only 8.1 in DMSO was reported for such aquacomplex (ref. 24b).
29 A. Gansäuer, L. Shi, M. Otte, I. Huth, A. Rosales, I. Sancho-Sanz, N. M. Padial and J. E. Oltra, *Radicals in Synthesis III. Topics in Current Chemistry*, ed. M. Heinrich, A. Gansäuer, Springer, Berlin, Heidelberg, 2011, pp. 93–120.
30 H. Toftlund, E. Pedersen and S. Yde-Andersen, *Acta Chem. Scand. A*, 1984, **38**, 693–697.
31 Nevertheless, a more complex situation was observed in DMSO-d_6 (See ESI, Fig. S2), in which new signals can be clearly observed. They can be attributed to partial dissociation of the chloride from the metal center or even to the equilibrium between different configurations in the complex: C. M. Coates, K. Hagan, C. A. Mitchell, J. D. Gorden and C. R. Goldsmith, *Dalton Trans.*, 2011, **40**, 4048–4058.
32 ^{1}H-NMR spectrum of a complex derived from the chloride-SbF_6 exchange also presents nine clear signals (see ESI, Figs. S13-S15), being also in qualitative agreement with the previous one. Therefore, an equilibrium between configurations can be in principle a fast process in NMR timescale.
33 R. L. Carlin, *Magnetochemistry*, Springer-Verlag. Berlin, 1986.
34 S. A. Cantalupo, S. R. Fiedler, M. P. Shores, A. L. Rheingold and L. H. Doerrer, *Angew. Chem. Int. Ed.*, 2012, **51**, 1000–1005.
35 M. E. Pascualini, N. V. Di Russo, A. E. Thuijs, A. Ozarowski, S. A. Stoian, K. A. Abboud, G. Christou and A. S. Veige, *Chem. Sci.*, 2015, **6**, 608–612.
36 R. Boča, *Coord. Chem. Rev.*, 2004, **248**, 757–815.
37 D. E. Freedman, W. H. Harman, T. D. Harris, G. J. Long, C. J. Chang and J. R. Long, *J. Am. Chem. Soc.*, 2010, **132**, 1224–1225.
38 (*a*) F. G. Bordwell, J.-P. Cheng and J. A. Harrelson Jr., *J. Am. Chem. Soc.*, 1988, **110**, 1229–1231; (*b*) D. D. M. Wayner and V. D. Parker, *Acc. Chem. Res*., 1993, **26**, 287–294; (*c*) J. W. Darcy, B. Koronkiewicz, G. A. Parada and J. M. Mayer, *Acc. Chem. Res.*, 2018, **51**, 2391–2399.
39 W. S. Matthews, J. E. Bares, J. E. Bartmess, F. G. Bordwell, F. J. Cornforth, G. E. Drucker, Z. Margolin, R. J. McCallum, G. J. McCollum and N. R. Vanier, *J. Am. Chem. Soc.*, 1975, **97**, 7006–7014.
40 F. G. Bordwell and W.-Z. Liu, *J. Am. Chem. Soc.*, 1996, **118**, 8777–8781.
41 To avoid this latter undesired ligand exchange process involving the chloride anion, we also measured the corresponding complex derived from the chloride-SbF_6 exchange possessing a less coordinative counteranion. As expected, this dicationic complex showed a lower pK_a value (24.0). This variation in only three units of pK_a seems reasonable taking into account the low Lewis acidity expected for Fe(II) complexes. Nevertheless, we were unable to obtain the corresponding single crystal X-ray structure of such complex and this result must be only considered under this perspective.
42 This pK_a decrease was also observed when less coordinating counter ions were present. In fact, complex derived from the chloride-SbF_6 exchange showed a pK_a value of 22.6. Again, we were unable to obtain the corresponding single crystal X-ray structure of such complex and this result must be only considered under this perspective.
43 R. L. Birke, C. Shi, W. Zhang and J. R. Lombardi, *J. Phys. Chem. B,* 1998, **102**, 7983–7996.
44 L. S. Morris, M. P. Girouard, M. H. Everhart, W. E. McClain, J. A. van Paridon, R. D. Pike and C. Goh, *Inorg. Chim. Acta*, 2014, **413**, 149–159.
45 S. Groni, C. Hureau, R. Guillot, G. Blondin, G. Blain and E. Anxolabéhère-Mallart, *Inorg. Chem.,* 2008, **47**, 11783–11797.
46 M. C. White, A. D. Doyle and E. N. Jacobsen, *J. Am. Chem. Soc*., 2001, **123**, 7194.
47 G. M. Sheldrick, *Acta Crystallogr. A*, 2015, **71**, 3–8.
48 G. M. Sheldrick, *Acta Crystallogr. A,* 2008, **64**, 112–122.
49 L. J. Farrugia, *J. Appl. Crystallogr.,* 2012, **45**, 849–854.
50 M. J. Frisch, G. W. Trucks, H. B. Schlegel, G. E. Scuseria, M. A. Robb, J. R. Cheeseman, G. Scalmani, V. Barone, B. Mennucci, G. A. Petersson, H. Nakatsuji, M. Caricato, X. Li, H. P. Hratchian, A. F. Izmaylov, J. Bloino, G. Zheng, J. L. Sonnenberg, M. Hada, M. Ehara, K. Toyota, R. Fukuda, J. Hasegawa, M. Ishida, T. Nakajima, Y. Honda, O. Kitao, H. Nakai, T. Vreven, J. A. Montgomery Jr., J. E. Peralta, F. Ogliaro, M. Bearpark, J. J. Heyd, E. Brothers, K. N. Kudin, V. N. Staroverov, T. Keith, R. Kobayashi, J. Normand, K. Raghavachari, A. Rendell, J. C. Burant, S. S. Iyengar, J. Tomasi, M. Cossi, N. Rega, J. M. Millam, M. Klene, J. E. Knox, J. B. Cross, V. Bakken, C. Adamo, J. Jaramillo, R. Gomperts, R. E. Stratmann, O. Yazyev, A. J. Austin, R. Cammi, C. Pomelli, J. W. Ochterski, R. L. Martin, K. Morokuma, V. G. Zakrzewski, G. A. Voth, P. Salvador, J. J. Dannenberg, S. Dapprich, A. D. Daniels, O. Farkas, J. B. Foresman, J. V. Ortiz, J. Cioslowski and D. J. Fox, Gaussian 09, Revision B.01, Gaussian, Inc., Wallingford CT 2010.
51 P. J. Hay and W. R. Wadt, *J. Chem. Phys.*, 1985, **82**, 270–283.
52 J. Tomasi, B. Mennucci and R. Cammi, *Chem. Rev.*, 2005, **105**, 2999–3094.

DOI: 10.1039/C8DT04689A

Coordination of hydroxyl/amide groups to Fe(II) diminishes BDFEs of O–H and (CO)N–H bonds down to 76.0 and 80.5 kcal mol^{-1} respectively.

View Article Online
DOI: 10.1039/C8DT04689A

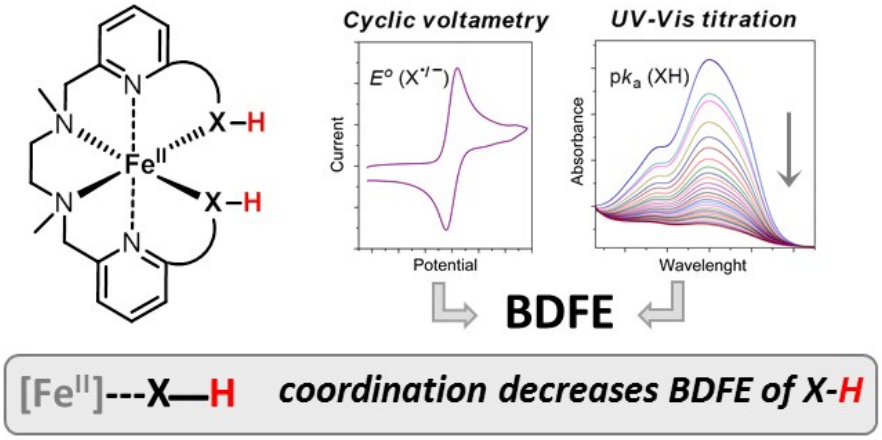

79x39mm (230 x 230 DPI)